Deep Atlantic carbon sequestration and atmospheric CO_2 decline during the last glaciation

J. Yu[1]*, L. Menviel[2,3], Z. Jin[4], D.J.R. Thornalley[5], S. Barker[6], G. Marino[1], E. J. Rohling[1,7], Y. Cai[4], F. Zhang[4], X. Wang[8], Yuhao Dai[1], Pujiao Chen[1], W. S. Broecker[9]

[1]Research School of Earth Sciences, The Australian National University, Canberra, ACT 2601, Australia

[2]Climate Change Research Centre, University of New South Wales, Sydney, Australia

[3]ARC Centre of Excellence for Climate System

[4]State Key Laboratory of Loess and Quaternary Geology, Institute of Earth Environment, Chinese Academy of Sciences, Xi'an 710075, China

[5]Dept. Of Geography, University College London, London, UK

[6]School of Earth and Ocean Sciences, Cardiff University, Cardiff, UK.

[7]Ocean and Earth Science, University of Southampton, National Oceanography Centre, Southampton SO14 3ZH, UK

[8]Earth Observatory of Singapore, Nanyang Technological University, 50 Nanyang Av., 639798, Singapore

[9]Lamont-Doherty Earth Observatory of Columbia University, 61 Route 9W/PO Box 1000, Palisades, NY, 10964-8000, USA

*Correspondence to: jimin.yu@anu.edu.au

Revised for *Nature Geoscience* on 10 September, 2015

A marked atmospheric CO_2 decline occurred ~70,000 years ago when Earth's climate descended into the last ice age [1,2], but its underlying causes remain enigmatic. We present the first quantification of changes in the carbon inventory of the deep Atlantic Ocean (>~3 km) during this time interval, based on deep water carbonate ion concentration ($[CO_3^{2-}]$) reconstructions for multiple sediment cores. A widespread $[CO_3^{2-}]$ decline of ~25 μmol/kg implies that the deep Atlantic carbon inventory increased by at least ~50 Gigatonnes, compared to the concomitant ~60 Gigatonnes carbon loss from the atmosphere [1,2]. Based on proxy observations and modeling [3], we infer that this carbon sequestration coincided with a shoaling of Atlantic meridional overturning circulation. Our evidence suggests that Atlantic Ocean circulation changes played an important role in atmospheric CO_2 reductions at the onset of the last glacial by increasing the carbon storage in the deep Atlantic.

Ice core records show a tight correlation between changes in atmospheric CO_2 and Antarctic temperature, suggesting an important role of atmospheric CO_2 fluctuations in affecting Earth's climate on orbital and millennial timescales [1,2]. During the last glacial cycle, a major climate change occurred at the Marine Isotope Stage (MIS) 5-4 transition around 70 thousand years ago (ka), manifested by a significant global cooling, a substantial build-up of polar ice sheets, and profound ocean circulation changes [2,4-7]. The atmospheric CO_2 decline across this transition accounts for about one third of the entire atmospheric CO_2 drawdown between full interglacial and glacial conditions [1,2]. Although the deep ocean is the widely suspected culprit for lowering glacial atmospheric CO_2 [8,9] probably through biogeochemical and physical processes

[3,6,10,11], convincing evidence for carbon sequestration in the deep ocean is limited, and the role of ocean circulation changes in enhanced deep-sea carbon storage remains elusive [3,6]. Here, we present a first quantification of carbon budget change in the deep Atlantic Ocean and investigate its relationship with changes in Atlantic Meridional Overturning Circulation (AMOC) across the MIS 5-4 transition.

Seawater carbonate ion concentration ($[CO_3^{2-}]$) is primarily governed by dissolved inorganic carbon (DIC) and alkalinity (ALK) (Fig. 1), and variations in other environmental parameters such as temperature and salinity only play a minor role [12,13]. Changes (Δ) in $[CO_3^{2-}]$, DIC and ALK can be approximated by

$$\Delta_{[CO_3^{2-}]} \approx k \times (\Delta_{ALK} - \Delta_{DIC}) \qquad (1)$$

where $k = 0.59 \pm 0.01$ (1σ; used throughout) (Supplementary Fig. 1, 2). Therefore, with sound knowledge about Δ_{ALK}, reconstructions of deep water $\Delta_{[CO_3^{2-}]}$ would allow an estimate of Δ_{DIC}, the term that ultimately determines the carbon budget change of the investigated ocean reservoir. Equation (1) successfully predicts seawater DIC in the modern deep Atlantic Ocean [14] (Fig. 1b).

We present deep water $[CO_3^{2-}]$ from ~90 to 50 ka for 10 sediment cores (6 new and 4 from [15,16]) retrieved from a wide geographic and depth range in the Atlantic Ocean (Fig. 1). Deep water $[CO_3^{2-}]$ are reconstructed using B/Ca in epifaunal benthic foraminifer *Cibicidoides wuellerstorfi*, with an uncertainty of ±5 μmol/kg for $[CO_3^{2-}]$ based on a core-top calibration [17] (Supplementary Fig. 3). The sediment-core age models are constructed by tuning all benthic $\delta^{18}O$ records to a single target curve, namely the LR04 global $\delta^{18}O$ stack [18] (Supplementary Fig. 4-6 and Table 1-3). The age ranges for MIS 5a (85-75 ka) and MIS 4 (59-69 ka) are based on light (<~3.3‰) and heavy (>~3.8‰) values in benthic $\delta^{18}O$, respectively. Detailed information on materials and methods is described in the Supplementary Information.

Fig. 2 shows that *C. wuellerstorfi* B/Ca in all 10 cores decreased from MIS 5a to MIS 4. Relative to mean MIS 5a values, deviations of B/Ca ($\Delta_{B/Ca}$) during MIS 4 are -20±5 μmol/mol (n=35) in 7 cores from the eastern basin and -42±11 μmol/mol (n=21) in 3 cores (EW9209-2JPC, RC16-59, and GeoB1118-3) from the western Atlantic (Fig. 3a-b; Supplementary Table 4). As discussed previously [17,19], *C. wuellerstorfi* B/Ca is minimally biased by postmortem dissolution, and we therefore attribute decreased B/Ca values during MIS 4 to reductions in deep Atlantic [CO_3^{2-}]. Based on the sensitivity of 1.14 μmol/mol per μmol/kg specific to *C. wuellerstorfi* derived from core tops[17], benthic $\Delta_{B/Ca}$ suggest 18±6 and 37±12 μmol/kg reductions in deep water [CO_3^{2-}] in the eastern and western basins, respectively (Fig. 3a). Considering data from all 10 cores together, benthic B/Ca decreased by 28±13 μmol/mol (n=56), corresponding to 25±13 μmol/kg decline in [CO_3^{2-}], from MIS 5a to MIS 4 (Fig. 3).

In contrast to different $\Delta_{B/Ca}$, benthic $\delta^{13}C$ exhibit similar amplitudes between cores at ~3.5 km water depth from the eastern (MD01-2446 and MD95-2039) and western (EW9209-2JPC and RC16-59) basins in the North Atlantic (Supplementary Fig. 7). One possibility for this contrast is that source waters ventilating the two basins during MIS 4 had different $\delta^{13}C$ endmembers. $\delta^{13}C$ heterogeneity of northern sourced waters has been previously reported for the Last Glacial Maximum[12,20]. At present, we attribute the larger $\Delta_{B/Ca}$ to a greater ocean circulation change in the western basin (Supplementary Fig. 8), in which case a higher source water $\delta^{13}C$ would be required for the west Atlantic during MIS 4. Future work is needed to explore reasons for the inter-basin $\Delta_{B/Ca}$ difference, but this uncertainty does not affect the conclusion of this study.

Benthic B/Ca and $\delta^{18}O$ are negatively correlated in each core (Supplementary Fig. 9-10). This suggests that the decrease in deep water $[CO_3^{2-}]$ into MIS 4 was associated with deep ocean cooling and the buildup of continental ice, which are thought to be linked to declining atmospheric CO_2 during the last glacial inception[1,2,4,21]. The overall pattern of changes in deep water $[CO_3^{2-}]$, based on a Monte-Carlo-style probabilistic assessment of the combined $[CO_3^{2-}]$ reconstructions of the 10 studied cores (Supplementary Information), displays a first order similarity to the evolution of atmospheric CO_2, in that both deep Atlantic $[CO_3^{2-}]$ and atmospheric CO_2 decreased from MIS 5a to MIS 4 [1,2] (Fig. 3c, d). This provides evidence to support previous suggestions [11,12,16,22] that changes in deep Atlantic carbonate chemistry must have played an important role in glacial-interglacial atmospheric CO_2 variations.

Because our data are from 10 sites that are widely distributed in the Atlantic (water depth: ~2.9 to 5 km, latitude: 41°S to 41°N) (Fig. 1), we consider that the 25±13 μmol/kg reduction in deep water $[CO_3^{2-}]$ approximates the mean $[CO_3^{2-}]$ variation for the whole deep Atlantic (>~3 km) from MIS 5a to 4 (Fig. 3a-c). As a cross-check, we use the $[CO_3^{2-}]$-$\delta^{13}C$ relationship and the mean deep Atlantic $\delta^{13}C$ change to infer the mean seawater $[CO_3^{2-}]$ decrease in the deep Atlantic across the MIS 5a-4 transition (Supplementary Fig. 11-12) . For the 10 cores studied, deep water $[CO_3^{2-}]$ is significantly correlated with benthic $\delta^{13}C$ ($r^2 = 0.50$, $P < 0.0001$), yielding a slope of 0.0228‰ per μmol/kg. A compilation study reveals that benthic $\delta^{13}C$ declined by an average of ~0.45‰ from MIS 5a to MIS 4 at numerous sites throughout the deep

Atlantic Ocean[23]. If the [CO_3^{2-}]-$\delta^{13}C$ relationship observed at our 10 geographically widely distributed sites is applicable to other locations in the deep Atlantic, then a 0.45‰ drop in $\delta^{13}C$ would suggest a ~20 μmol/kg reduction in deep water [CO_3^{2-}], falling within the uncertainty of 25±13 μmol/kg calculated based on [CO_3^{2-}] reconstructions for the 10 studied cores (Fig. 3a-c).

Four lines of evidence suggest that the lowered deep water [CO_3^{2-}] during MIS 4 is not caused by a drop in ALK, but by an increase in DIC in the deep Atlantic. First, when [CO_3^{2-}] declines, deep water becomes more corrosive and that would enhance water-column and deep-sea $CaCO_3$ dissolution, a process that drives up oceanic ALK [9,12]. In the preindustrial Atlantic, the decreasing [CO_3^{2-}] from North Atlantic Deep Water (NADW) to Antarctic Bottom Water (AABW) was accompanied by a rise in deep water ALK (Fig. 1d) [14]. As shown both in our studied cores (Fig. 2) and at other locations in the deep Indo-Pacific Oceans (e.g., [24,25]), global deep-sea $CaCO_3$ dissolution dramatically intensified (i.e., the lysocline shoaled) from MIS 5a to MIS 4, with a likely effect of raising the global ocean ALK inventory [9,12]. Second, the ~50 m sea level drop into MIS 4 [4] would have substantially reduced the shelf area for neritic carbonate deposition, which in turn would have raised the oceanic ALK [26]. Third, benthic Ba/Ca ratios, a proxy used to reflect deep water ALK [27], show no decrease during MIS 4 at four locations in the Atlantic Ocean (Supplementary Fig. 13). Fourth, model studies show higher ocean ALK in glacials than in interglacials [11,28] (Supplementary Information).

We first assume no change in ALK (i.e., $\Delta_{ALK} = 0$) to quantify the magnitude of deep water DIC increase (Fig. 3b; Supplementary Information), and subsequently evaluate how this assumption affects the conclusions. Based on Equation (1), a 25±13 μmol/kg decline in deep water [CO_3^{2-}] translates into a 42±22 μmol/kg increase in DIC. Using a mass of 10.1×10^{19} kg for waters below 3 km in the Atlantic, we calculate that a total amount of 51±27 Gt (1 Gt = 1×10^{15} g) extra carbon was sequestered in the deep Atlantic during the transition from MIS 5a to 4 (Fig. 3c). During this period, atmospheric CO_2 declined by 28±11 ppm (MIS 5a: 237±8 ppm; MIS 4: 208±8 ppm), corresponding to a loss of 60±23 Gt carbon from the atmosphere [1,2] (Fig. 3d). Therefore, the carbon stock increase in the deep Atlantic, in quantity, is equivalent to ~86±56% of the contemporary atmospheric CO_2 drawdown across the MIS 5a-4 transition.

Note that the deep Atlantic carbon budget change calculated above represents a conservative estimate. CO_2 sequestration in the deep ocean across MIS 5a-4 would inevitably raise deep water acidity, lower seawater [CO_3^{2-}], and consequently intensify deep-sea $CaCO_3$ dissolution (Fig. 2). This so called deep-sea carbonate compensation (Supplementary Information) serves as a negative feedback to restore the global deep water [CO_3^{2-}] to the initial level, on a time scale of ~5-7,000 years, via raising the whole ocean ALK until the global ocean ALK input (from mainly continental weathering) reaches a new steady state with ALK output (by shelf and deep-sea carbonate burials) [9,12,19,29-31]. The effect of carbonate compensation may be manifested by partial reversals of [CO_3^{2-}] in MD01-2446, EW9209-2JPC, and RC16-59 (Fig. 2). However, none of the studied [CO_3^{2-}] records returned to the MIS 5a levels within the ~10,000 year duration of MIS 4. In numerical models, deep Atlantic [CO_3^{2-}] remains low for ~8,000 years after a weakening or shutdown of NADW (Supplementary Fig. 15, 19). The sustained low [CO_3^{2-}] during MIS 4 suggests that processes within the Atlantic must impose a stronger control on the deep water acidity than the opposing effect from a global ocean ALK rise. Without a global ALK increase due to carbonate compensation, a much larger [CO_3^{2-}] decrease would be expected in the deep Atlantic. Given a reconstructed deep water [CO_3^{2-}] reduction, Equation (1) suggests that for every unit increase in ALK the DIC increase would be one unit higher than the number calculated assuming Δ_{ALK} = 0. This is demonstrated by distributions of carbon species in today's Atlantic Ocean (Fig. 1) [14]: to account for the ~40 μmol/kg [CO_3^{2-}] reduction between NADW ([CO_3^{2-}]= ~120 μmol/kg) and AABW ([CO_3^{2-}] = ~80 μmol/kg), Equation (1) would predict a $\Delta_{DIC_{AABW-NADW}}$ of ~68 μmol/kg if no change in ALK, which is ~38% smaller than the observed DIC change (Fig. 1c). The difference is caused by a ~40 μmol/kg ALK increase from NADW to AABW (Fig. 1d). Had the pre-industrial $\Delta_{[CO_3^{2-}]}$:Δ_{DIC} ratio of -0.37 been applied, which empirically includes the ALK changes (Fig. 3c), then our calculated deep Atlantic carbon storage increase would be amplified by a factor of 1.6, and the quantity of carbon sequestration in the deep Atlantic would be comparable within uncertainty to the entire atmospheric CO_2 decline from MIS 5a to MIS 4. Additionally, consideration of larger $\Delta_{B/Ca}$ in the western Atlantic, which is currently under sampled (Fig. 3a), would potentially raise the estimate of carbon sequestration in the deep Atlantic.

Enhanced carbon storage in the deep Atlantic during MIS 4 may have resulted from synergistic physical and biogeochemical processes [9,11]. Regarding physical processes, sediment neodymium isotopes (εNd; an ocean circulation proxy) imply an increased contribution of CO_2-rich southern-sourced abyssal waters (Fig. 1) in the deep Atlantic at the MIS 5a-4 transition [3,32]. During MIS 4, the NADW-AABW boundary probably shoaled to ~2-3 km water depth, and was located above major topographic ridges and seamounts [6,32]. Such a rearrangement of the AMOC would weaken diapycnal mixing between water masses, enhance water column stratification, and thereby facilitate the retention of sequestered carbon in the deep ocean [5,33]. In core TNO57-21, a sharp ~1ε unit increase in εNd at ~70 ka [3] exactly coincided with a rapid ~12 μmol/kg decline in deep water $[CO_3^{2-}]$ inferred from benthic B/Ca (Fig. 4). Because seawater $[CO_3^{2-}]$ is primarily determined by DIC and ALK, both of which place direct constraints on the oceanic carbon cycle [9,11,29,31], synchronous changes in εNd and B/Ca indicate a tight coupling between AMOC and carbon cycling in the deep Atlantic during the last glaciation. The earlier ~0.5‰ decrease in benthic foraminiferal $\delta^{13}C$ (Fig. 4b) [34], which was previously used to infer global carbon budget change leading an AMOC reorganization [3], might be caused by air-sea isotopic exchange effects [35]. The coupling of AMOC and carbon cycling is corroborated by results from two Earth system models of intermediate complexity: halving the NADW formation leads to 10-30 μmol/kg reductions in $[CO_3^{2-}]$ below ~3 km in the deep Atlantic without causing anoxia in the deep ocean (Supplementary Fig. 22-23). Regarding the biogeochemistry, the decreased deep Atlantic $[CO_3^{2-}]$ during MIS 4 is consistent with a more efficient biological pump in the glacial Southern Ocean perhaps stimulated by increased iron availability [10] and a greater water column remineralization due to stagnant AMOC [6,7,32], both of which would increase sequestration of respiratory DIC into the ocean interior and decrease atmospheric CO_2 [9,11,36].

Our calculations highlight that, despite its relatively modest proportion (~30%) of the global deep ocean volume, the deep Atlantic sequestered a substantial amount of carbon during the onset of the last glaciation around 70 ka, especially when concomitant ALK increase is taken into account. The sequestered amount is quantitatively comparable to the contemporary carbon loss from the atmosphere. We also find that this large carbon sequestration was tightly coupled with AMOC changes. The movements of carbon between reservoirs in the atmosphere - land biosphere - ocean system are intricately linked, and future studies should aim to quantify the contributions from individual sources to the increased carbon storage in the deep ocean during glaciations.

References:

1. Ahn, J. & Brook, E. J. Atmospheric CO(2) and climate on millennial time scales during the last glacial period. *Science* **322**, 83-85 (2008).
2. Bereiter, B. et al. Mode change of millennial CO2 variability during the last glacial cycle associated with a bipolar marine carbon seesaw. *Proceedings of the National Academy of Sciences of the United States of America* **109**, 9755-9760 (2012).
3. Piotrowski, A., Goldstein, S. J., Hemming, S. R. & Fairbanks, R. G. Temporal Relationships of carbon cycling and ocean circulation at glacial boundaries. *Science* **307**, 1933-1938 (2005).
4. Grant, K. M. et al. Rapid coupling between ice volume and polar temperature over the past 150,000 years. *Nature*, doi:10.1038/nature11593 (2012).
5. Adkins, J. F. The role of deep ocean circulation in setting glacial climates. *Paleoceanography* **28**, 539-561 (2013).
6. Thornalley, D. J. R., Barker, S., Becker, J., Hall, I. R. & Knorr, G. Abrupt changes in deep Atlantic circulation during the transition to full glacial conditions. *Paleoceanography* **28**, 253-262 (2013).
7. Barker, S. & Diz, P. Timing of the descent into the last ice age determined by the bipolar seesaw. *Paleoceanography* (2014).
8. Broecker, W. Glacial to interglacial changes in ocean chemistry. *Progr. Oceanogr.* **2**, 151-197 (1982).
9. Sigman, D. M. & Boyle, E. A. Glacial/interglacial variations in atmospheric carbon dioxide. *Nature* **407**, 859-869 (2000).
10. Martinez-Garcia, A. et al. Iron Fertilization of the Subantarctic Ocean During the Last Ice Age. *Science* **343**, 1347-1350 (2014).
11. Hain, M. P., Sigman, D. M. & Haug, G. H. Carbon dioxide effects of Antarctic stratification, North Atlantic Intermediate Water formation, and subantarctic nutrient drawdown during the last ice age: Diagnosis and synthesis in a geochemical box model. *Global Biogeochemical Cycles* **24** (2010).
12. Yu, J. M., Elderfield, H. & Piotrowski, A. Seawater carbonate ion-$\delta^{13}C$ systematics and application to glacial-interglacial North Atlantic ocean circulation. *Earth and Planetary Science Letters* **271**, 209-220. doi:10.1016/j.epsl.2008.04.010 (2008).
13. Zeebe, R. E. & Wolf-Gladrow, D. A. *CO_2 in Seawater: Equilibrium, Kinetics, Isotopes* (ed. Halpern, D.) (Elsevier, Amsterdam, 2001).
14. Key, R. M. et al. A global ocean carbon climatology: Results from Global Data Analysis Project (GLODAP). *Global Biogeochemical Cycles* **18** (2004).
15. Broecker, W., Yu, J. & Putnam, A. E. Two contributors to the glacial CO_2 decline. *Earth and Planetary Science Letters*, http://dx.doi.org/10.1016/j.epsl.2015.07.019 (2015).
16. Raitzsch, M., Hathorne, E. C., Kuhnert, H., Groeneveld, J. & Bickert, T. Modern and late Pleistocene B/Ca ratios of the benthic foraminifer Planulina wuellerstorfi determined with laser ablation ICP-MS. *Geology* **39**, 1039-1042 (2011).
17. Yu, J. M. & Elderfield, H. Benthic foraminiferal B/Ca ratios reflect deep water carbonate saturation state. *Earth and Planetary Science Letters* **258**, 73-86, doi: 10.1016/j.epsl.2007.03.025 (2007).
18. Lisiecki, L. E. & Raymo, M. E. A Pliocene-Pleistocene stack of 57 globally distributed benthic $\delta^{18}O$ records. *Paleoceanography* **20**, PA1003, doi:10.1029/2004PA001071 (2005).

19. Yu, J. et al. Deep South Atlantic carbonate chemistry and increased interocean deep water exchange during last deglaciation. *Quaternary Science Reviews* (2014).
20. Repschlager, J., Weinelt, M., Andersen, N., Garbe-Schonberg, D. & Schneider, R. Northern source for Deglacial and Holocene deepwater composition changes in the Eastern North Atlantic Basin. *Earth and Planetary Science Letters* **425**, 256-267 (2015).
21. Elderfield, H. et al. Evolution of Ocean Temperature and Ice Volume Through the Mid-Pleistocene Climate Transition. *Science* **337**, 704-709 (2012).
22. Hodell, D. A., Charles, C. D. & Sierro, F. J. Late Pleistocene evolution of the ocean's carbonate system. *Earth and Planetary Science Letters* **192**, 109-124 (2001).
23. Oliver, K. I. C. et al. A synthesis of marine sediment core delta C-13 data over the last 150 000 years. *Climate of the Past* **6**, 645-673 (2010).
24. Le, J. & Shackleton, N. J. Carbonate dissolution fluctuations in the Western equatorial Pacific during the late Quaternary. *Paleoceanography* **7**, 21-42 (1992).
25. Howard, W. R. & Prell, W. L. Late Quaternary $CaCO_3$ production and preservation in the Southern Ocean - Implications for oceanic and atmospheric carbon cycling. *Paleoceanography* **9**, 453-482 (1994).
26. Ridgwell, A. J., Watson, A. J., Maslin, M. A. & Kaplan, J. O. Implications of coral reef buildup for the controls on atmospheric CO_2 since the Last Glacial Maximum. *Paleoceanography* **18** (2003).
27. Lea, D. & Boyle, E. Barium content of benthic foraminifera controlled by bottom- water composition. *Nature* **338**, 751-753 (1989).
28. Toggweiler, J. R. Origin of the 100,000-year timescale in Antarctic temperatures and atmospheric CO_2. *Paleoceanography* **23**, PA2211, doi:10.1029/2006PA001405 (2008).
29. Broecker, W. S. & Peng, T. H. The role of $CaCO_3$ compensation in the glacial to interglacial atmospheric CO_2 change. *Global Biogeochemical Cycles* **1**, 15-29 (1987).
30. Emerson, S. & Archer, D. Glacial carbonate dissolution cycles and atmospheric pCO_2: A view from the ocean bottom. *Paleoceanography* **7**, 319-331 (1992).
31. Marchitto, T. M., Lynch-Stieglitz, J. & Hemming, S. R. Deep Pacific $CaCO_3$ compensation and glacial-interglacial atmospheric CO_2. *Earth and Planetary Science Letters* **231**, 317-336 (2005).
32. Bohm, E. et al. Strong and deep Atlantic meridional overturning circulation during the last glacial cycle. *Nature* **517**, 73-U170 (2015).
33. Ferrari, R. et al. Antarctic sea ice control on ocean circulation in present and glacial climates. *Proceedings of the National Academy of Sciences of the United States of America* **111**, 8753-8758 (2014).
34. Ninnemann, U. S. & Charles, C. D. Changes in the mode of Southern Ocean circulation over the last glacial cycle revealed by foraminiferal stable isotopic variability. *Earth And Planetary Science Letters* **201**, 383-396 (2002).
35. Lynch-Stieglitz, J., Stocker, T. F., Broecker, W. & Fairbanks, R. G. The influence of air-sea exchange on the isotopic composition of oceanic carbon: Observations and modeling. *Global Biogeochemical Cycles* **9**, 653-665 (1995).
36. Menviel, L., Joos, F. & Ritz, S. P. Simulating atmospheric CO_2, ^{13}C and the marine carbon cycle during the Last Glaciale/Interglacial cycle: possible role for a deepening of the mean remineralization depth and an increase in the oceanic nutrient inventory. *Quaternary Science Reviews* **56**, 46-68 (2012).

Acknowledgments. We thank Daniel Sigman, Bob Anderson, Barbel Hönisch, and two anonymous reviewers for insightful and constructive discussions and comments, and Les Kinsley and Laura Rodriguez-Sanz for laboratory assistance. This work is supported by ARC Discovery Project (DP140101393) and Future Fellowship (FT140100993) to JY, DECRA (DE150100107) to LM, and by Australian Laureate Fellowship (FL120100050) to EJR. Core materials were kindly provided by LDEO (Nichole Anest), NOC (Guy Rothwell, and WHOI (Ellen Roosen/Delia Oppo) core repositories. Model experiments were performed on a computational cluster owned by the Faculty of Science of the University of New South Wales as well as on a cluster from the NCI National Facility at the Australian National University.

Author contributions. JY designed and performed the research and wrote the paper; LM carried out modeling; ZJ/FZ picked foram shells; DJRT/SB and YD/PC generated data for MD95-2039 and EW9209-2JPC/RC16-59, respectively; GM/EJR conducted MC simulation; all authors contributed to improving the manuscript.

Additional information. Supplementary information is available in the online version of the paper. Reprints and permissions information is available online at www.nature.com/reprints. Correspondence and requests for materials should be addressed to J.Y.

Competing financial interests. The authors declare no competing financial interests.

Figure 1 | Atlantic Ocean carbonate chemistry and sediment cores. **a**, Locations of the studied sediment cores (circles) against meridional distributions of preindustrial DIC (color shading, μmol/kg) and $[CO_3^{2-}]$ (contours, μmol/kg) in the Atlantic Ocean. a = MD95-2039 (40.6°N, 10.3°W, 3,381 m), b = MD01-2446 (39°N, 12.6°W, 3,576 m), c = EW9209-2JPC (5.6°N, 44.5°W, 3,528 m), d = RC16-59 (4.0°N, 43.0°W, 3,520 m), e = GEOB1115-3 (3.56°S, 12.56°W, 2,945 m), f = GEOB1117-2 (3.81°S, 14.89°W, 3,984 m), g = GEOB1118-3 (3.56°S, 16.42°W, 4,671 m), h = RC13-228 (22.3°S, 11.2°E, 3,204 m), i = RC13-229 (25.5°S, 11.3°E, 4,191 m), j = TNO57-21 (41.1°S, 7.8°E, 4,981 m), NADW = North Atlantic Deep Water, AABW = Antarctic Bottom Water. Bottom-right inset shows the transect of hydrographic data used for mapping by Ocean Data View (http://odv.awi-bremerhaven.de). **b,** Predicted DIC by ALK and [CO_3^{2-}] using Equation (1) vs. measured DIC (Supplementary Information). **c,** DIC vs. [CO_3^{2-}]. **d,** ALK vs. [CO_3^{2-}]. In **b-d,** data are for the deep Atlantic Ocean (water depth: > 2.5 km, latitude: 70°S- 70°N, longitude: 15°E-65°W, n = 3327), and the red lines represent linear regressions. The blue line in **c** shows the DIC trend expected from [CO_3^{2-}] based on Equation (1), assuming no change in ALK. Hydrographic data are from the GLODAP dataset [14].

Figure 2 | Reconstructed [CO_3^{2-}] in the deep Atlantic (>~3 km) across the MIS 5-4 transition. **a,** MD95-2039 (square) and MD01-2446 (circle). **b,** EW9209-2JPC (square) and RC16-59 (circle) (ref. [15] and this study). **c,** GeoB1115-3 (circle)[16], GeoB1117-2 (triangle)[16] and GeoB1118-3 (square)[16]. To facilitate displaying data in the same plot, B/Ca from GeoB1115-3 and GeoB1118-3 are shifted by -20 μmol/mol and +40 μmol/mol, respectively. The [CO_3^{2-}] scale is only for core GeoB1117-2. **d,** RC13-228. **e,** RC13-229. **f,** TNO57-21. *C. wuellerstorfi* B/Ca is converted to deep water [CO_3^{2-}] using a sensitivity of 1.14 μmol/mol per μmol/kg [17]. Unless mentioned, all B/Ca are from this study. Age models for cores are based on comparisons of benthic $\delta^{18}O$ with the LR04 curve [18] (Supplementary Fig. 4). Vertical orange and cyan shadings represent MIS 5a and MIS 4, respectively. Grey lines represent sediment carbonate contents (%$CaCO_3$).

Figure 3 | Deep Atlantic carbon budget across the MIS 5-4 transition. **a,** Histogram and average values (squares ± 1σ) of *C. wuellerstorfi* $\Delta_{B/Ca}$ (deviations of individual measurements from the $B/Ca_{MIS\ 5a}$ mean) for MIS 5a (red) and MIS 4 (green: eastern basin; grey: western basin; black: all cores). The upper abscissa shows the corresponding change in $[CO_3^{2-}]$, $\Delta_{[CO_3^{2-}]}$, using a sensitivity of 1.14 μmol/mol per μmol/kg [17]. **b,** Temporal evolution of $\Delta_{B/Ca}$ and $\Delta_{[CO_3^{2-}]}$ in 10 cores. The minimum Δ_{DIC} is calculated by Equation (1) assuming no increase in seawater ALK (Supplementary Information). **c,** Monte-Carlo-style probabilistic assessment of $[CO_3^{2-}]$ changes shown in **b**, with the bold curve showing the probability maximum and the shaded envelope giving its 95% probability interval (Supplementary Information). The minimum change in total carbon, $\Delta_{\sum carbon}$, in the deep Atlantic is estimated using a mass of 10.1×10^{19} kg for the deep Atlantic Ocean (>~3 km), and its equivalent quantity expressed in terms of changes in atmospheric CO_2 is scaled by 1 ppm atmospheric CO_2 = 2.1 GtC. **d,** Atmospheric CO_2 [1,2].

Figure 4 | Temporal evolution of geochemical proxies in core TNO57-21 from the deep South Atlantic. **a,** Sediment εNd, an ocean circulation proxy [3]. **b,** Benthic $\delta^{13}C$ [34], a geochemical tracer influenced by a combination of processes including ocean circulation, biogenic remineralization, and air-sea exchange, not all of which are associated with a change in the deep ocean DIC. **c,** Benthic B/Ca (this study), a proxy for deep water $[CO_3^{2-}]$ which reflects changes in DIC and ALK, both of which are tightly linked to the carbon cycle in the ocean. The high sedimentation rate (~15 cm/kyr) in TNO57-21 through the 65-75 ka interval significantly minimizes bioturbation influences on geochemical tracers.

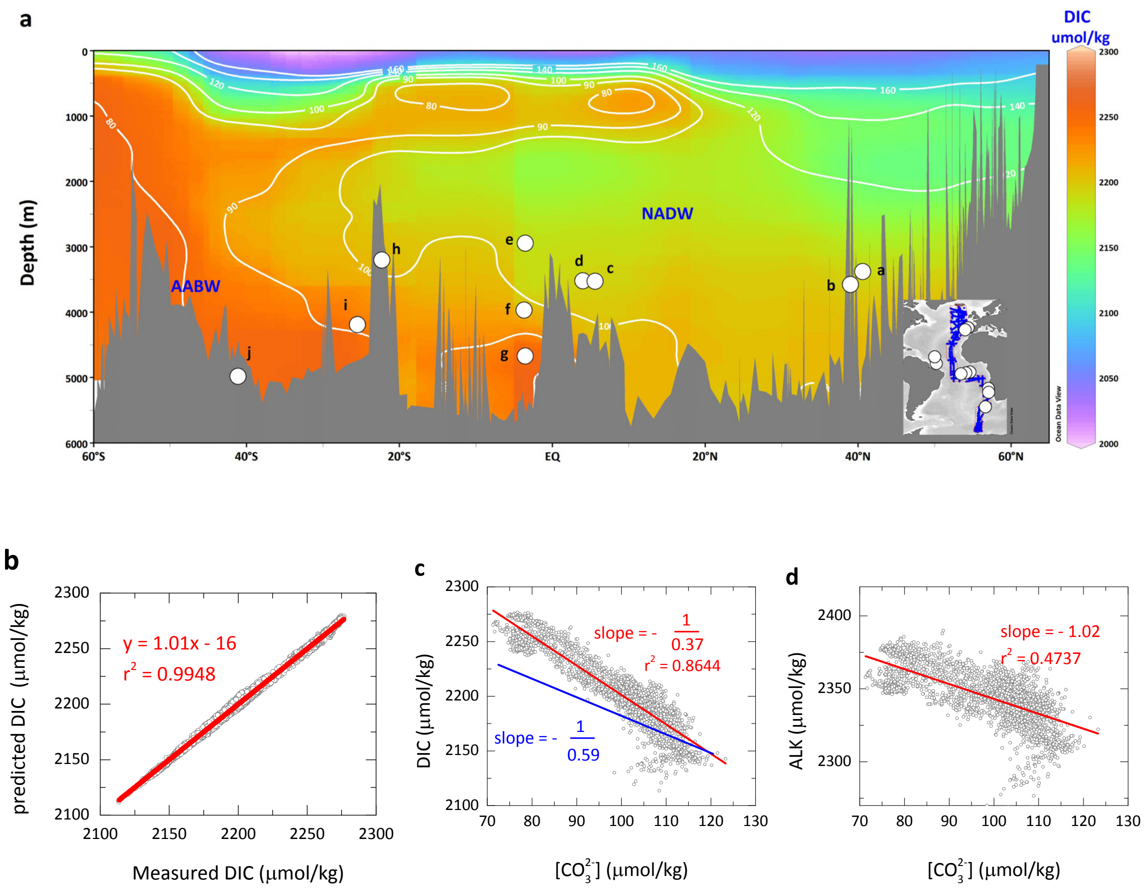
a
DIC
umol/kg
Depth (m)
AABW
NADW
60°S
40°S
20°S
EQ
20°N
40°N
60°N
Ocean Data View
b
predicted DIC (μmol/kg)
Measured DIC (μmol/kg)
y = 1.01x - 16
r2 = 0.9948
c
DIC (μmol/kg)
[CO32-] (μmol/kg)
slope = - 1/0.37
r2 = 0.8644
slope = - 1/0.59
d
ALK (μmol/kg)
[CO32-] (μmol/kg)
slope = - 1.02
r2 = 0.4737

Figure 1

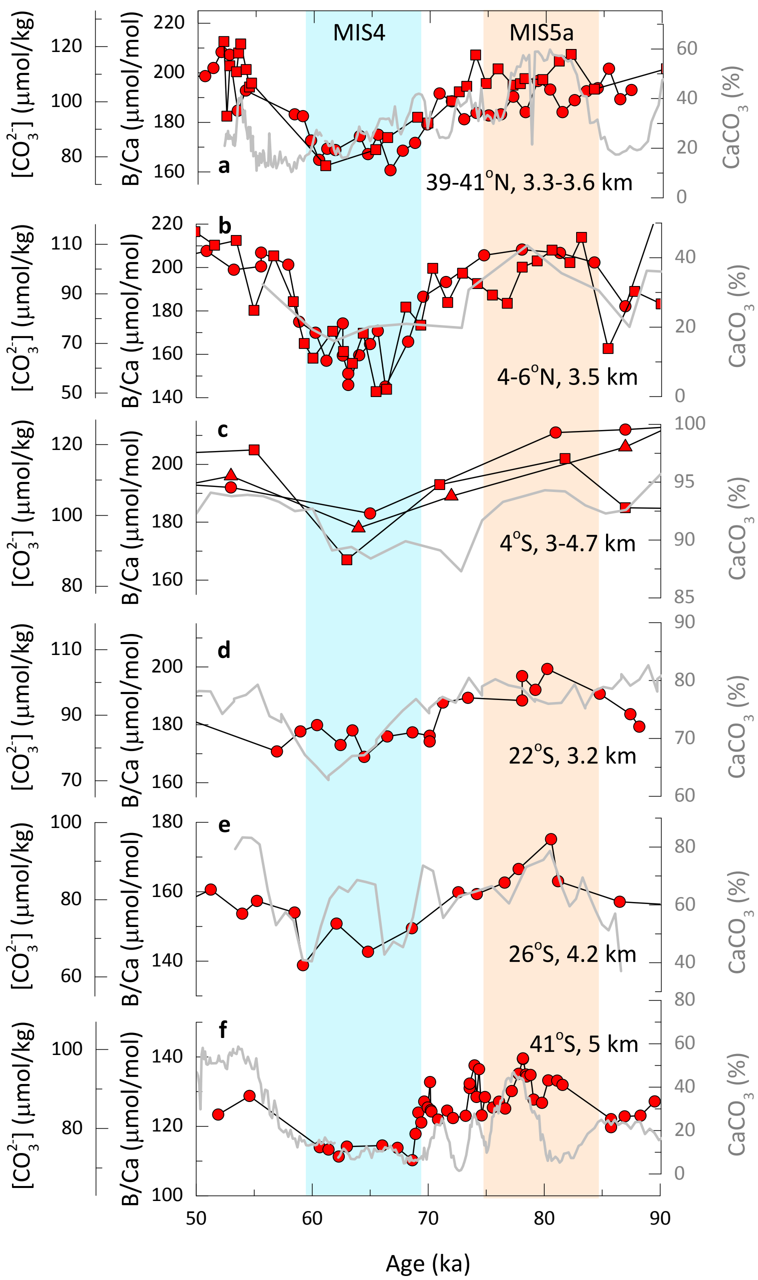
MIS4
MIS5a
a
39-41°N, 3.3-3.6 km
b
4-6°N, 3.5 km
c
4°S, 3-4.7 km
d
22°S, 3.2 km
e
26°S, 4.2 km
f
41°S, 5 km
[CO32-] (µmol/kg)
B/Ca (µmol/mol)
CaCO3 (%)
Age (ka)
50
60
70
80
90

Figure 2

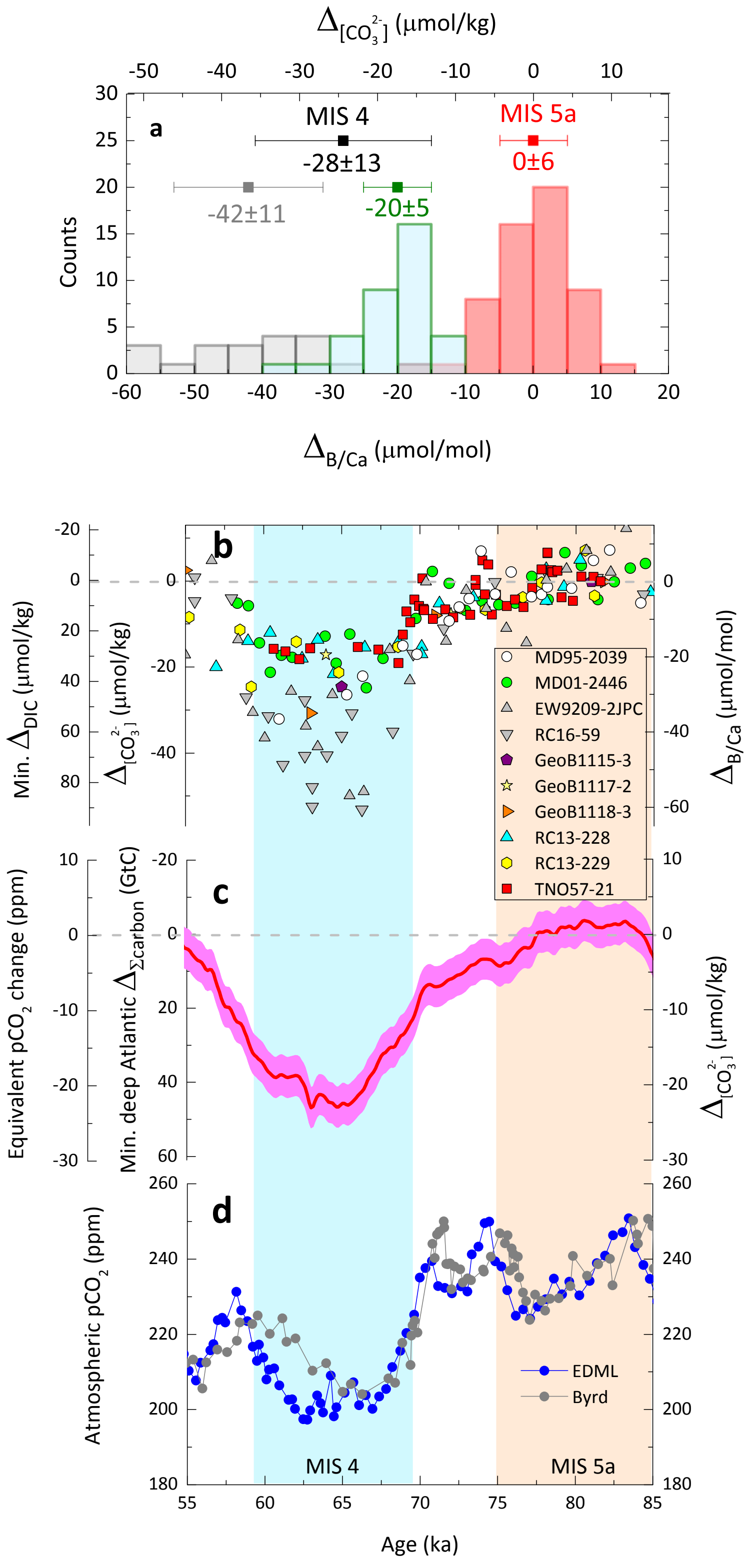

a
MIS 4
-28±13
-42±11
-20±5
MIS 5a
0±6
Counts
$\Delta_{[CO_3^{2-}]}$ (μmol/kg)
$\Delta_{B/Ca}$ (μmol/mol)
b
Min. Δ_{DIC} (μmol/kg)
$\Delta_{[CO_3^{2-}]}$ (μmol/kg)
$\Delta_{B/Ca}$ (μmol/mol)
MD95-2039
MD01-2446
EW9209-2JPC
RC16-59
GeoB1115-3
GeoB1117-2
GeoB1118-3
RC13-228
RC13-229
TNO57-21
c
Equivalent pCO$_2$ change (ppm)
Min. deep Atlantic $\Delta_{\Sigma carbon}$ (GtC)
$\Delta_{[CO_3^{2-}]}$ (μmol/kg)
d
Atmospheric pCO$_2$ (ppm)
EDML
Byrd
MIS 4
MIS 5a
Age (ka)

Figure 3

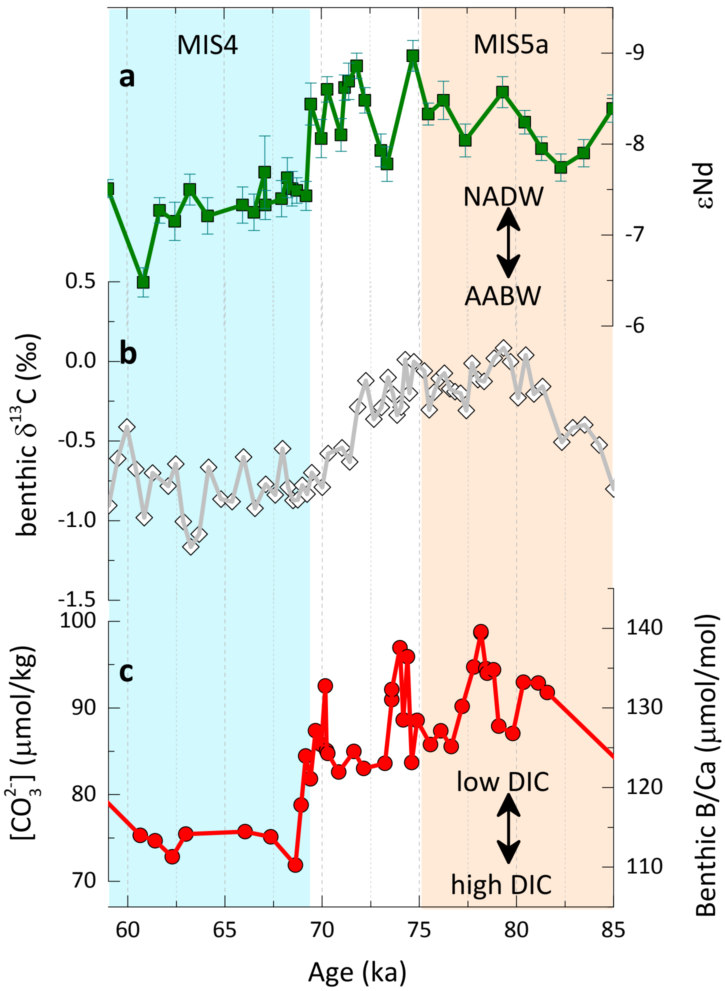
MIS4
MIS5a
a
b
c
NADW
AABW
low DIC
high DIC
εNd
benthic δ13C (‰)
[CO32-] (µmol/kg)
Benthic B/Ca (µmol/mol)
Age (ka)
-9
-8
-7
-6
0.5
0.0
-0.5
-1.0
-1.5
100
90
80
70
140
130
120
110
60
65
70
75
80
85

Figure 4